FEBS Letters

FEBS PRESS science publishing by scientists

Environmental pH and a Glu364 to Gln mutation in the chlorophyll-binding CP47 protein affect redox-active TyrD and charge recombination in Photosystem II

Jaz N. Morris[1,2], Sándor Kovács[3], Imre Vass[3], Tina C. Summerfield[1] and Julian J. Eaton-Rye[2]

1 Department of Botany, University of Otago, Dunedin, New Zealand
2 Department of Biochemistry, University of Otago, Dunedin, New Zealand
3 Institute of Plant Biology, Biological Research Centre, Hungarian Academy of Sciences, Szeged, Hungary

Correspondence
J. J. Eaton-Rye, Department of Biochemistry, University of Otago, PO Box 56, Dunedin 9054, New Zealand
Fax: +63 3 479 7865
Tel: +64 3 479 7866
E-mail: julian.eaton-rye@otago.ac.nz

(Received 24 September 2018, revised 19 November 2018, accepted 19 November 2018, available online 18 December 2018)

doi:10.1002/1873-3468.13307

Edited by Richard Cogdell

In Photosystem II, loop E of the chlorophyll-binding CP47 protein is located near a redox-active tyrosine, Y_D, forming a symmetrical analog to loop E in CP43, which provides a ligand to the oxygen-evolving complex (OEC). A Glu364 to Gln substitution in CP47, near Y_D, does not affect growth in the cyanobacterium *Synechocystis* sp. PCC 6803; however, deletion of the extrinsic protein PsbV in this mutant leads to a strain displaying a pH-sensitive phenotype. Using thermoluminescence, chlorophyll fluorescence, and flash-induced oxygen evolution analyses, we demonstrate that Glu364 influences the stability of Y_D and the redox state of the OEC, and highlight the effects of external pH on photosynthetic electron transfer in intact cyanobacterial cells.

Keywords: CP47; cyanobacteria; oxygen-evolving complex; Photosystem II; *Synechocystis* sp. PCC 6803; TyrD; Y_D

Photosystem II (PS II) is a light-driven water-plastoquinone oxidoreductase. In PS II, excitation of the four-chlorophyll P_{680} reaction center (RC) initiates a series of electron transfer steps *via* pheophytin to the primary and secondary plastoquinone acceptors (Q_A and Q_B, respectively) forming plastoquinol (Q_BH_2): these reactions are accompanied by the sequential extraction of electrons from water to fill the hole on P_{680} *via* a bound Mn_4CaO_5 oxygen-evolving complex (OEC) [1]. The PS II core complex includes the chlorophyll-binding antenna proteins CP43 and CP47 which are found adjacent to the RC proteins D1 and D2, respectively. In cyanobacteria, the PS II core is surrounded by 13 low molecular weight, membrane-spanning subunits and capped by up to four hydrophilic subunits on the lumenal face of the photosystem [2–4]. A similar arrangement among the peripheral subunits is found in eukaryotic organisms and the PS II core is conserved [5,6].

Two redox-active tyrosine residues, Y_Z (D1 Tyr161) and Y_D (D2 Tyr160), are located in symmetrical positions around P_{680} [1,7]. During photosynthetic electron

Abbreviations
CAPS, 3-(cyclohexylamino)-1-propanesulfonic acid; CP43, 43-kDa chlorophyll-binding core antenna protein; CP47, 47-kDa chlorophyll-binding core antenna protein; D1, PsbA reaction center protein; D2, PsbD reaction center protein; DCMU, 3,4-dichloro-1,1-dimethyl urea; F, fluorescence; F_O, dark-adapted (minimum) fluorescence; F_M, maximum level of fluorescence; HEPES, 4-(2-hydroxyethyl)-1-piperazineethanesulfonic acid; His_D, His189 of D2; His_Z, His190 of D1; OEC, oxygen-evolving complex; P_{680}, reaction center chlorophylls of PS II; P_{700}, reaction center chlorophylls of PS I; PCC, Pasteur Culture Collection; PS II, Photosystem II; Q_A primary plastoquinone electron acceptor of PS II; PS I, Photosystem I; Q_B, secondary plastoquinone electron acceptor of PS II; S_0–S_4, oxidation states of the OEC; *Synechocystis* 6803, *Synechocystis* sp. PCC 6803; TL, thermoluminescence; Y4/Y3, ratio of the O_2 yield on flash 4 to the O_2 yield on flash 3; $Y_D^{(ox)}$, oxidized form of Y_D (either Y_D^+ or the neutral radical $Y_D^{\cdot}$); Y_D, redox-active Tyr160 of the D2 protein; Y_Z, redox-active Tyr161 of the D1 protein.

transfer, Y_Z forms a neutral radical by movement of the phenolic proton toward a nearby His residue, called His_Z (D1 His190). Although an analogous His residue is found adjacent to Y_D (His_D or D2 His189) the formation of the neutral Y_D radical is mediated through a water molecule that is thought to connect to a proton exit pathway involving D2 Arg180 [8–10]. Upon excitation of PS II, Y_Z is oxidized by P_{680} and then rapidly reduced (within μs) by the OEC through a series of S state transitions (where S_0–S_4 denote oxidation states of the OEC); in contrast, oxidized Y_D ($Y_D^{(ox)}$) is stable for minutes and is not involved in water oxidation directly, but is involved in charge equilibrium with the OEC [1,10–13]. Although S_0 is the most reduced OEC state, S_1 is the dark-stable state, due to the reduction of $Y_D^{(ox)}$ to yield S_1Y_D OEC centers [10,14].

Both CP43 and CP47 possess six membrane-spanning helices joined by hydrophilic loops (loops A–E). In both proteins loop E is a large lumenal loop, comprising ~ 130 amino acids in CP43 and ~ 190 residues in CP47 [15]. While Glu354 and Arg357 of Loop E from CP43 are in the first and second coordination spheres of the OEC, respectively, a conserved Phe362-Phe363-Glu364 region in loop E of CP47 contributes to a hydrophobic pocket around Y_D [3]. This hydrophobic pocket (Fig. 1) is thought to be important for the formation of the hydrogen bond network surrounding Y_D that permits electron transfer from Y_D to P_{680}^+; accordingly, the hydrophobic pocket may also reduce damaging charge recombination from the PS II acceptor side (*via* the P_{680} RC) to the $Y_D^{\cdot}$ radical, because of the lack of an available proton [9,10]. Glu364 is within H-bonding distance (~ 2.8 Å) to D2 Arg294, which coordinates His_D [10,16], and this residue might therefore be important for the release of the phenolic proton of Y_D to the available water [8,9,17]. However, in the cyanobacterium *Synechocystis* sp. PCC 6803 (hereafter *Synechocystis* 6803), CP47 Glu364 to Gln or Glu364 to Gly substitutions produced strains similar to the wild-type, in contrast to severely impaired growth in a Phe363 to Arg mutant [18–21]. Loop E of CP47 extends into the thylakoid lumen and is involved in binding of the cyanobacterial PS II extrinsic subunit PsbO, which, along with the PsbU, PsbV, and possibly CyanoQ proteins, protects the OEC and Y_D from the reductive environment of the lumen and is necessary for maximal rates of oxygen evolution [2,22]. Deletion of PsbV in the CP47 E364Q mutant of *Synechocystis* 6803 resulted in a strain displaying a pH-sensitive phenotype, in which PS II function and assembly were reduced and photoautotrophic growth was not possible at pH 7.5; however, pH 10.0 rescued growth and PS II function [23,24].

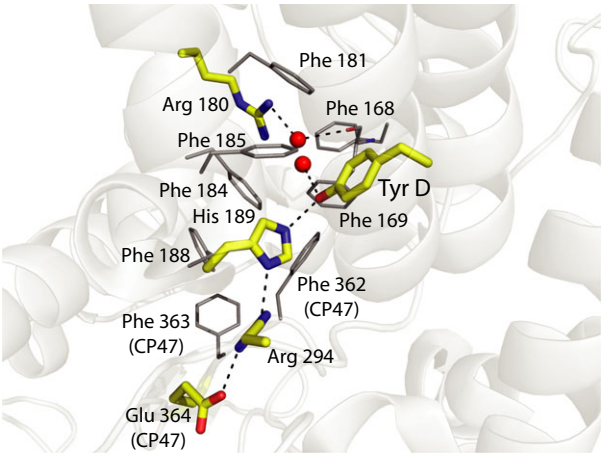

Fig. 1. Putative hydrogen bond network associated with Y_D of Photosystem II. The hydrophobic pocket surrounded by D2 Phe residues and Phe362 and Phe363 of CP47 is also depicted. The hypothesized hydrogen bond between CP47 Glu364 and D2 Arg294 is shown. The red spheres are the proximal and distal positions (with respect to the phenolic group of Y_D) of a single water located in the pocket. This water has been suggested to participate in proton coupled electron transfer when Y_D is oxidized by transferring the proton to D2 Arg180 [8,9]. The figure was drawn using PyMOL [52] and PDB 4UB6 [16].

A number of pH-sensitive PS II mutants of *Synechocystis* 6803 carrying deletions in PS II extrinsic proteins have been reported [23–27], despite the physical separation of the thylakoid lumen from changes in environmental pH. To investigate possible mechanisms for this phenomenon [28], and with recent studies highlighting Glu364 as an important residue in the Y_D pocket [9,17,29], we were prompted to look again at the E364Q mutant in the context of possible redox perturbations around Y_D. In the case of the pH 7.5 nonphotoautotrophic E364Q:ΔPsbV strain, we hypothesized that an altered environment around Y_D at pH 7.5 compounds the contribution of PsbV removal to pH sensitivity. Thus, we investigated PS II activity in the E364Q and E364Q:ΔPsbV mutants, compared to wild-type and the ΔPsbV strain. By determination of thermoluminescence (TL), chlorophyll *a* (hereafter chlorophyll) fluorescence decay measurements, and flash-induced oxygen production, we demonstrate that CP47 Glu364 is important for charge recombination in PS II, and suggest a mechanism by which altered Y_D oxidation contributes to the pH-sensitivity of the E364Q:ΔPsbV mutant.

Materials and methods

Strains and culture conditions

Glucose-tolerant *Synechocystis* 6803 strains used in this work are listed in Table 1, and were grown using BG-11 liquid and solid media [30] in the presence of 5 mM glucose (unless indicated otherwise) and appropriate antibiotics, and maintained at 30 °C under continuous ~ 40 $\mu E \cdot m^{-2} \cdot s^{-1}$ illumination as described previously [31]. For physiological measurements, liquid cultures in mid-late logarithmic growth phase were harvested by centrifugation at ~ 2500 ***g***, washed twice with BG-11, and resuspended in BG-11 media buffered with either 25 mM HEPES-NaOH pH 7.5 or 25 mM CAPS-NaOH pH 10.0. Cells were incubated at 5 μg chlorophyll·mL^{-1} until the initiation of measurements, after 8 or 24 h, as appropriate to the experiment. For some measurements of flash-induced oxygen evolution, 5 mM glucose was added during the incubation period.

Physiological measurements

Measurement of TL was carried out using a custom-built machine [32,33]. For determination of TL, cells were subjected to 30 s of 250 $\mu E \cdot m^{-2} \cdot s^{-1}$ illumination at 20 °C and 3 min dark adaptation at 20 °C prior to cooling to −20 °C, whereupon a single-turnover actinic flash was provided by a xenon flash bulb. Samples were cooled to −40 °C, and subsequently warmed to 80 °C at a rate of 20 °C·min^{-1}, during which time the TL photon yield was measured. Measurements were made in the presence and absence of 20 μM 3,4-dichloro-1,1-dimethyl urea (DCMU), which was applied during the dark adaptation period. Data were analyzed by curve fitting to determine peak amplitude and peak temperatures using custom-made software, as in Ref. [34].

Flash-induced oxygen evolution was determined using a custom-built Joliot-type electrode [35] as described previously [36]. Briefly, intact cells (equivalent to 2.5 μg chlorophyll) were dark adapted for 5 min in direct contact with a bare platinum cathode and illuminated with saturating single-turnover actinic flashes provided by a 617 nm LED array. Twenty flashes at 4 Hz were used, with a flash width of 4–8 μs.

Table 1. *Synechocystis* sp. PCC 6803 strains used in this work.

Strain	References	Antibiotics added to BG-11 plate culture
Wild-type GT-O1	[53,54]	–
E364Q	[20]	Kanamycin 25 μg·mL^{-1}
ΔPsbV	[20]	Erythromycin 25 μg·mL^{-1}
E364Q:ΔPsbV	[20]	Kanamycin 25 μg·mL^{-1} and Erythromycin 25 μg·mL^{-1}

Details about the creation of mutant strains and the GT-O1 wild-type are available in the references indicated.

Room temperature chlorophyll fluorescence decay and induction measurements using cells dark adapted for 5 min prior to measurements were made using an FL-3000 double-modulation fluorimeter (Photon Systems Instruments, Brno, Czech Republic) using parameters previously described [37]. Fluorescence decay measurements were made in the presence and absence of 20 μM DCMU added in the dark adaptation period, and fluorescence decay data were analyzed using the software ORIGIN 2017 (OriginLab, MA, USA), using a fitting algorithm previously described [34,38].

The PS I oxidation state in cells was determined by P_{700}-dependent absorbance changes in the near-infrared ($A_{875\ nm}-A_{830\ nm}$) induced by illumination with 635 nm actinic light (~ 1000 $\mu E \cdot m^{-2} \cdot s^{-1}$) [39] using a Dual-PAM-100 measuring system (Walz, Effeltrich, Germany). Cells were dark adapted for 5 min prior to measurements, and data were baseline corrected and normalized to the P_{700}^{+} oxidation state maxima.

Results

pH, and the Glu364 to Gln substitution, affects thermoluminescence yield and C band stability

To assess the effects of the Glu364 to Gln mutation and pH on charge recombination in PS II, *Synechocystis* 6803 strains were incubated under photoautotrophic conditions at pH 7.5 and pH 10.0 for 8 h, and the TL from these strains was determined. In dark-adapted PS II following a single-turnover actinic flash, charge recombination produces characteristic TL bands from $S_2Q_B^-$ (B band), $S_2Q_A^-$ (Q band—occurs in the presence of DCMU), and $Y_D^{(ox)}Q_A^-$ (C band—may occur whether DCMU is present or not) charge pairs [32,34,40,41]. The wild-type and the ΔPsbV, E364Q, and E364Q:ΔPsbV strains typically displayed enhanced TL yield from B and Q bands at pH 7.5 compared to pH 10.0, and increased C band yield (in the presence and absence of DCMU) at pH 10.0 compared to pH 7.5, indicating increased charge recombination between the quinone acceptors and the OEC at low pH and increased recombination between $Y_D^{(ox)}$ and Q_A^- at higher pH (Fig. 2, Table 2). However, the B band TL yield was similar at both pH values for wild-type and the B band yield was larger at pH 10 than pH 7.5 in E364Q cells (Fig. 2A; Table 2). In addition, in the presence of DCMU, the intensity of the C band in the ΔPsbV strain was somewhat larger at pH 7.5 than at pH 10 while the C band was similar at both pH values in E364Q:ΔPsbV cells (Fig. 2D, Table 2). Strikingly, the E364Q mutant emitted B, Q, and C band TL at a much greater level than wild-type

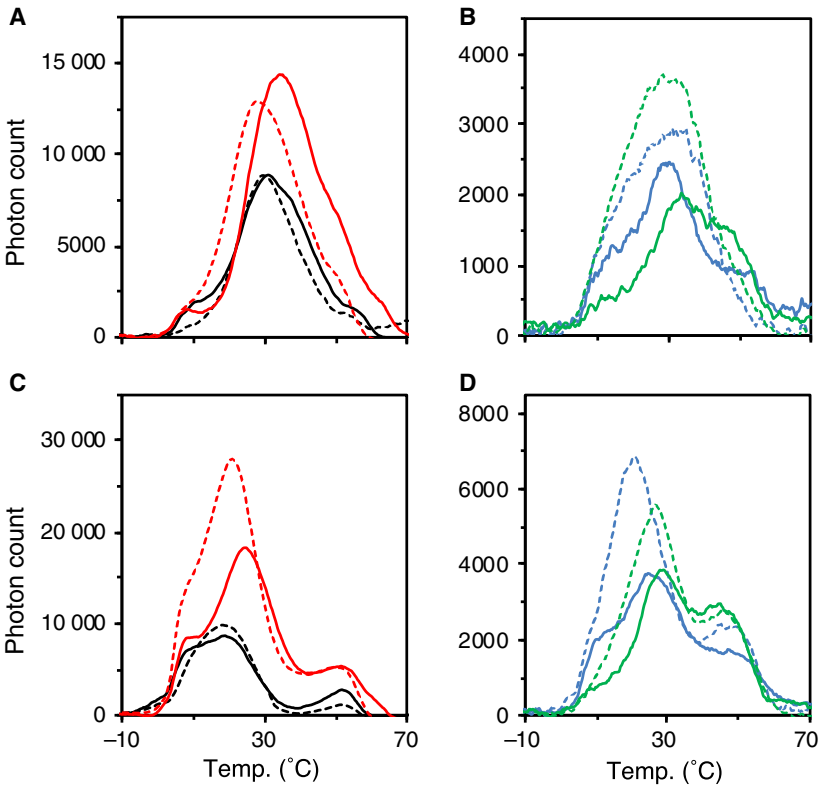

Fig. 2. Thermoluminescence from *Synechocystis* sp. PCC 6803 strains incubated for 8 h in pH 7.5 (dashed lines) or pH 10.0 (solid lines) under photoautotrophic conditions. Measurements were made in the absence (panels A and B) and presence (panels C and D) of DCMU. Traces represent the mean photon count from three to five independent measurements. (A, C) Wild-type = black, E364Q = red. (B, D) ΔPsbV = blue, and E364Q:ΔPsbV = green.

cells, and both mutants lacking PsbV had reduced TL yield, likely due to reduced PS II levels in these strains [23]. Moreover, C band yield was enhanced in E364Q:ΔPsbV cells in the presence of DCMU compared to ΔPsbV cells, indicating an increased population of $Y_D^{(ox)}Q_A^-$ in these mutants. Furthermore, the temperatures of TL peak maxima (T_{max}, which indicates the activation energy required to cause charge recombination and hence charge pair stability) were similar for B and Q bands in wild-type, and for the B band in the

Table 2. Temperature of TL peak maxima (T_{max}) and relative peak amplitude of *Synechocystis* sp. PCC 6803 strains.

		− DCMU		+ DCMU	
Strain	Growth pH	B band T_{max} (°C) (amplitude)	C band T_{max} (°C) (amplitude)	Q band T_{max} (°C) (amplitude)	C band T_{max} (°C) (amplitude)
Wild-type	pH 7.5	30.25 ± 2.2 (8060 ± 1669)	51.7 ± 2.4 (1549 ± 737)	20.2 ± 0.5 (10451 ± 288)	52.65 ± 0.2 (1750 ± 263)
	pH 10.0	32.2 ± 1.7 (7810 ± 682)	54.15 ± 0.9 (2397 ± 1170)	20.0 ± 1.7 (9212 ± 461)	53.15 ± 0.89 (3296 ± 1183)
E364Q	pH 7.5	32 ± 1.1 (11065 ± 9266)	50.1 ± 0.9 (5257 ± 3553)	21.7 ± 0.7 (29990 ± 7604)	50.5 ± 1.6 (6925 ± 1413)
	pH 10.0	34.3 ± 1.7 (15082 ± 1755)	55.1 ± 4.7 (6312 ± 2520)	25.3 ± 0.9 (19401 ± 8550)	53.8 ± 4.6 (7224 ± 4798)
ΔPsbV	pH 7.5	29.8[a] (3070)	48.1[a] (550)	23.0[a] (6474)	48.7[a] (2329)
	pH 10.0	29.7[a] (2481)	49.2[a] (901)	26.6 ± 4.8 (3894 ± 969)	51.8 ± 3.8 (1846 ± 1046)
E364Q:ΔPsbV	pH 7.5	28.7 ± 0.2 (3831 ± 1189)	49.65 ± 1.6 (986 ± 115	26.91 ± 0.8 (5599 ± 2024)	46.6 ± 1 (2931 ± 673)
	pH 10.0	37.1 ± 6.8 (2133 ± 840)	51.4[a] (1547)	29.5 ± 1.0 (3774 ± 1579)	46.4 ± 0.7 (2936 ± 1451)

Growth conditions: strains were assayed after 8 h in pH 7.5/pH 10.0 photoautotrophic conditions in the absence and presence of DCMU (mean ± SEM, n = 3–5). [a]Fit based on a single curve due to signal to noise in these cells.

ΔPsbV strain, between pH levels, but both mutants carrying the Glu364 to Gln substitution showed enhanced B and Q band stability at pH 10.0. Compared to the wild-type, all mutants showed enhanced Q band T_{max} ($S_2Q_A^-$ stability), with an apparent additive effect from the Glu364 to Gln substitution and removal of PsbV in the E364Q:ΔPsbV double mutant. Similar to TL yield, the C band T_{max} was generally enhanced at pH 10.0 in the presence and absence of DCMU, indicating an increase in $Y_D^{(ox)}Q_A^-$ stability at higher pH.

The Glu364 to Gln substitution impairs back reactions of PS II independently of the PsbV deletion

Chlorophyll fluorescence decay following a single-turnover actinic flash can be used to probe reoxidation of Q_A^- in PS II by Q_B or by the OEC [34,42], and was measured in tandem with TL (Fig. 3, Table 3). In wild-type cells, the chlorophyll decay kinetics consist of a fast phase (μs) reflecting the oxidation of Q_A^- by bound Q_B, a medium phase (ms) that is thought to arise from Q_A^- oxidation in centers where Q_B was not bound before the actinic flash and a slow phase (s) which corresponds to the back reaction with the S_2 state of the OEC [38]. At pH 7.5 the fast phase of the fluorescence decay was slightly slowed in the E364Q cells when compared to wild-type but the medium phase was similar, suggesting the Q_B binding site properties were also similar in wild-type and the E364Q mutant. In contrast, the slow phase in the E364Q strain exhibited a $t_{1/2}$ of 9.5 s compared to 1.3 s in the wild-type although both had similar amplitudes (Table 3). A similar trend was seen between these two strains when the chlorophyll decay was measured in cells grown and measured at pH 10.0 but in this instance the amplitude of the slow phase increased from 15% to 18% in the E364Q cells while it decreased in wild-type to 11%.

The chlorophyll fluorescence decay kinetics in the ΔPsbV strain also exhibited slowed fast and slow components relative to wild-type; however, the ΔPsbV strain also had a slowed middle phase (e.g., from 1.5 ms in wild-type to 5.1 ms in ΔPsbV cells at pH 7.5 and a similar change was evident at pH 10.0; Table 3).

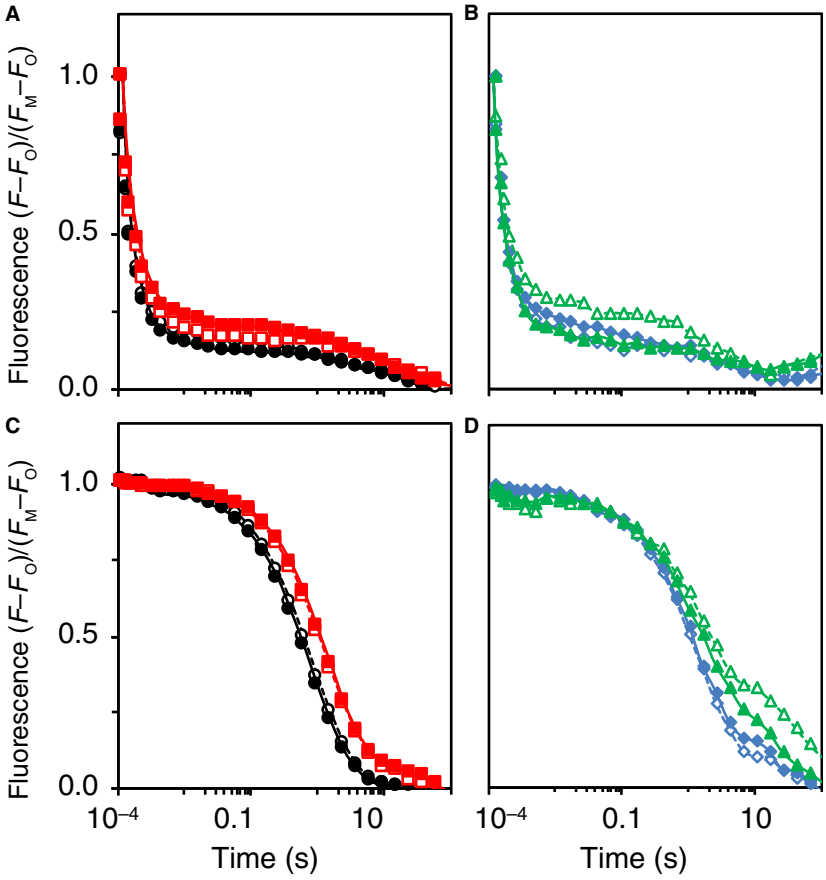

Fig. 3. Fluorescence decay following a single-turnover actinic flash in *Synechocystis* sp. PCC 6803 strains incubated for 8 h in pH 7.5 (dashed lines) or pH 10.0 (solid lines) under photoautotrophic conditions. Measurements were made in the absence (panels A and B) and presence (panels C and D) of DCMU. Traces represent the mean of three to five independent measurements. (A, C) Wild-type = black, E364Q = red. (B, D) ΔPsbV = blue, and E364Q:ΔPsbV = green.

Table 3. Kinetics of single-turnover flash-induced chlorophyll fluorescence decay in *Synechocystis* sp. PCC 6803 strains.

Strain	Growth pH	+/− DCMU	Fast phase $t_{1/2}$ (μs) [amp (%)]	Medium phase $t_{1/2}$ (ms) [amp (%)]	Slow phase $t_{1/2}$ (s) [amp (%)]
Wild-type	7.5	−	174 ± 17 (50 ± 4.9)	1.5 ± 0.4 (35 ± 5.9)	1.3 ± 0.11 (15 ± 1.8)
	10.0	−	213 ± 16 (59 ± 1.4)	1.7 ± 0.1 (30 ± 2.5)	4.3 ± 1.28 (11 ± 2.1)
	7.5	+		2.5 ± 0.9 (2.3 ± 0.4)	0.6 ± 0.04 (98 ± 0.4)
	10.0	+		1.3 ± 0.3 (3.1 ± 1.1)	0.6 ± 0.04 (97 ± 1.1)
E364Q	7.5	−	253 ± 18 (54 ± 3.8)	2.1 ± 0.2 (31 ± 2.8)	9.5 ± 3.99 (15 ± 2.6)
	10.0	−	252 ± 20 (49 ± 3.7)	1.9 ± 0.3 (32 ± 2.5)	7.0 ± 3.49 (18 ± 1.8)
	7.5	+		4.1 ± 2.3 (2.9 ± 1.7)	1.1 ± 0.08 (97 ± 1.7)
	10.0	+		0.5 ± 0.2 (2.1 ± 0.4)	1.2 ± 0.03 (98 ± 0.4)
ΔPsbV	7.5	−	288 ± 14 (68 ± 3.4)	5.1 ± 2.0 (19 ± 5.2)	7.1 ± 4.82 (12 ± 3.0)
	10.0	−	259 ± 56 (57 ± 7.8)	4.5 ± 1.6 (24 ± 9.4)	6.1 ± 2.47 (19 ± 7.9)
	7.5	+		5.3 ± 4.9 (5.2 ± 2.2)	1.0 ± 0.09 (95 ± 2.2)
	10.0	+		5.1 ± 3.3 (8.9 ± 6.6)	1.0 ± 0.01 (91 ± 6.6)
E364Q:ΔPsbV	7.5	−	216 ± 31 (40 ± 8.7)	1.6 ± 0.5 (36 ± 6.6)	2.5 ± 0.93 (24 ± 7.8)
	10.0	−	165 ± 21 (46 ± 6.5)	1.3 ± 0.2 (43 ± 9.0)	1.5 ± 0.27 (10 ± 3.6)
	7.5	+		0.2 ± 0.1 (8.8 ± 2.5)	1.3 ± 0.11 (91 ± 2.1)
	10.0	+		0.7 ± 0.3 (7.1 ± 2.7)	1.5 ± 0.19 (93 ± 2.7)

Growth conditions: strains were grown to mid-late log-phase, incubated for 8 h in pH 7.5/photoautotrophic or pH 10.0/photoautotrophic conditions, and assayed in the absence and presence of DCMU (shaded rows). In the absence of DCMU, fast phase decay occurs due to Q_A^- to Q_B electron transfer in the presence of bound Q_B, medium phase decay represents Q_A^- to Q_B electron transfer where Q_B was not bound, and slow phase decay is due to charge recombination of $S_2Q_A^-/Q_B^-$. Fluorescence decay in the presence of DCMU, due to occupation of the Q_B site by DCMU, primarily occurs due to charge recombination of $S_2Q_A^-$. Half times ($t_{1/2}$) and amplitudes (amp) were determined by curve fitting and are the average (± SEM) of three to five independent measurements.

Strikingly the E364Q:ΔPsbV double mutant exhibited kinetics more closely resembling the wild-type than either single mutant although the slow component at pH 7.5 had an elevated amplitude (24% in E364Q:ΔPsbV cells; 15% in wild-type) and there was a corresponding decrease in the amplitude of the fast component in the E364Q:ΔPsbV strain (Table 3).

In the presence of DCMU, the decay of chlorophyll fluorescence can be fit by a millisecond component and a slow seconds component [38]. In Table 3, the slow component is extended by approximately a factor of 2 relative to wild-type in all mutants and a slowed decay is observed in Fig. 3C,D. A large pH effect on the fast phase, however, was evident in E364Q cells [4.1 ms (3%) at pH 7.5 and 0.5 ms (2%) at pH 10.0]. The millisecond component in wild-type by comparison was 2.5 ms (2%) at pH 7.5 and 1.3 ms (3%) at pH 10.0, while in the ΔPsbV strain it remained constant at approximately 5 ms but with a slightly increased amplitude at pH 10.0 (Table 3). Interestingly, in the case of the E364Q:ΔPsbV double mutant, the millisecond component more closely resembled the rate observed at pH 10.0 for the E364Q strain (Table 3). In addition, when PsbV was absent, the chlorophyll decays did not reach zero and this effect was most pronounced in the E364Q:ΔPsbV mutant in the presence of DCMU at pH 7.5 (Fig. 3B,D). This suggests a reduced dark S_1 stable fraction of the OEC in ΔPsbV and E364Q:ΔPsbV cells.

The dark S state population of PS II is altered by the removal of PsbV and the Glu364 to Gln substitution

In order to assess the redox state of the PS II OEC following dark adaptation, measurements of flash-induced oxygen evolution were made using a Joliot-type electrode. In one experiment, wild-type and mutant cells were incubated for 24 h in pH 7.5 mixotrophic conditions permissive for growth in all strains (Fig. 4A). Charge recombination during 5 min of dark adaptation leads to a population of PS II with mixed OEC S states of around 25% $S_0Y_D^{(ox)}$/75% S_1Y_D [14]; thus, a distinct peak in oxygen evolution occurs following three single-turnover flashes (from OEC centers in an initial dark S_1 state), and a somewhat reduced 4th flash yield (initial S_0 state). In wild-type, a typical flash-induced oxygen evolution pattern was observed. However, a shift in the relative oxygen evolution favoring 4th flash oxygen evolution in cells lacking PsbV was observed with an increase in the S_0 population observed in both ΔPsbV and E364Q:ΔPsbV cells relative to wild-type and the E364Q strain, respectively (Table 4). Impaired photoautotrophic growth and

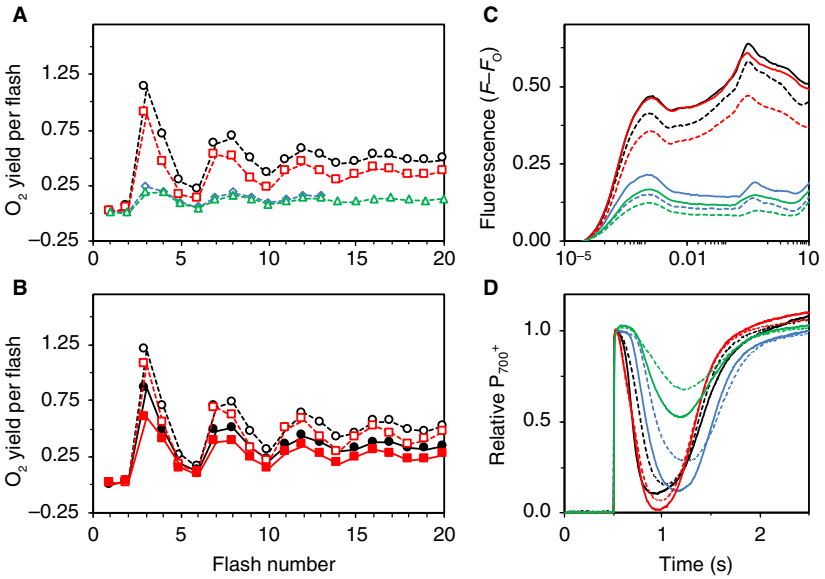

Fig. 4. Flash-induced oxygen evolution (panels A and B), fluorescence induction (panel C), and P_{700} oxidation state (panel D) of *Synechocystis* sp. PCC 6803 strains. Cells were incubated for 24 h (panel A) and 8 h (panels C and D) in pH 7.5 (dashed lines) or pH 10.0 (solid lines) under mixotrophic conditions, or incubated for 24 h in pH 7.5 in photoautotrophic conditions (panel B). (A, B) Flash-induced oxygen evolution during exposure of dark-adapted cells to 20 saturating, single-turnover actinic flashes at 617 nm/4 Hz. A representative trace following three to four independent measurements is shown; data were normalized to the first flash value. Flash-induced oxygen evolution was not measured for ΔPsbV and E364Q:ΔPsbV cells under photoautotrophic conditions. In panel A, the data for the first 13 flashes are plotted for the ΔPsbV mutant due to the noise arising as a result of the reduced number of PS II centers in these cells. (C) Fluorescence induction following the exposure of dark-adapted cells to actinic 639-nm light; traces represent the mean of three to four independent measurements. (D) P_{700} oxidation was induced after 0.5 s by exposure of dark-adapted cells to actinic 635-nm light; values reflect absorbance change in the near-infrared ($A_{875\ nm}$−$A_{830\ nm}$), and were normalized to the signal maxima (~ 100% P_{700}^+) and represent the mean of three to four independent measurements. In all panels the strains are: wild-type (black), E364Q (red), ΔPsbV (blue), and E364Q:ΔPsbV (green). In panel A and B the symbols are: wild-type, black circles; E364Q, red squares; ΔPsbV, blue diamonds, and E364Q:ΔPsbV, green triangles. In panel B empty symbols are pH 7.5 and filled symbols are pH 10.

oxygen evolution in strains lacking the PsbV protein meant that flash oxygen yield comparisons in pH 7.5/10.0 photoautotrophic conditions were made only in the wild-type and E364Q strains in a subsequent experiment (Fig. 4B). As in the case of mixotrophic growth, flash oxygen yields were somewhat reduced in the E364Q mutant compared to wild-type, in particular at pH 10.0. Although the normalized 4th flash/3rd flash yield from the wild-type was similar between pH levels, the yield from the E364Q strain compared to wild-type was apparently more variable, reduced at pH 7.5, and elevated at pH 10.0 (Table 4). In comparison to wild-type, the S_0 state was also increased in E364Q cells at both pH values (Table 4) revealing an increased population of a dark S_0 state in the E364Q mutant, rather than S_1.

The analysis of the oxygen evolution parameters in Table 4 additionally found the level of misses and double hits to be similar between the strains under mixotrophic conditions; however, under photoautotrophic conditions, E364Q cells exhibited a reduction in misses at pH 7.5 and an increase in double hits at pH 10.0. Furthermore, the number of active PS II centers in the dark-adapted cells, in any of the strains, was reduced relative to wild-type in the mixotrophically grown cells and the number of active centers at pH 10.0 relative to pH 7.5 in both wild-type and the E364Q strain declined. It should be noted that steady-state oxygen evolution and PS II assembly have been shown to be similar in wild-type and E364Q cells at pH 7.5 and pH 10.0 but the removal of PsbV (in cells grown at pH 7.5 or in unbuffered BG-11) in either background reduced the number of PS II centers by approximately 55% and 65%, respectively [20,23,27].

The Glu364 to Gln substitution does not substantially alter room temperature PS II fluorescence induction or low-temperature fluorescence; pH alters the rate of reduction of PS I

Variable chlorophyll fluorescence arising from PS II was induced in dark-adapted cells by actinic light;

Table 4. Analysis of the S state distribution under different growth conditions and at pH 7.5 or pH 10.0.[a]

Strain and treatment	S_0[b] (%)	S_1 (%)	S_2 (%)	S_3 (%)	Misses [α] (%)	Double hits [β] (%)	$\sum S_{i,dark}$[b] (a.u.)	Y4/Y3[c]
Mixotrophic growth at pH 7.5[d]								
Wild-type	17.0	83.0	0	0	15.9	3.1	1.00	0.608
ΔPsbV	29.6	70.4	0	0	15.7	2.1	0.24	0.820
E364Q	10.0	90.0	0	0	15.0	2.8	0.59	0.490
E364Q:ΔPsbV	33.5	66.5	0	0	16.1	2.4	0.20	1.133
Photoautotrophic growth[d]								
Wild-type pH 7.5	16.1	83.9	0	0	14.3	2.0	0.96	0.564
Wild-type pH 10	14.0	86.0	0	0	14.7	2.6	0.70	0.583
E364Q pH 7.5	19.0	81.0	0	0	11.2	2.2	0.78	0.515
E364Q pH 10	24.2	78.8	0	0	14.1	7.2	0.55	0.660

[a]Oxygen evolution parameters were fit by using the matrix formalism of the Joliot–Kok model of O_2 evolution[11,55] in combination with a least square minimizing simplex algorithm. [b]$S_0 \ldots S_3$ is the distribution of the S states in the dark and $\sum S_{i,dark}$ is the total number of active centers in any of the S states in the dark. [c]Ratio of the O_2 yield on flash 4 to the O_2 yield on flash 3. [d]Strains were grown in pH 7.5/mixotrophic conditions, and wild-type and E364Q strains grown in photoautotrophic pH 7.5 and pH 10.0 conditions, for 24 h. The comparison of the fitted flash-induced oxygen evolution data to the experimental measurements is shown for the mixotrophically grown cells in Fig. S1 and for the photoautotrophically grown cells in Fig. S2.

wild-type and E364Q cells showed a typical fluorescence induction 'OJIP' curve [43,44]. Greater variable fluorescence was observed in all strains at pH 10.0 relative to pH 7.5 following 8 h of incubation, particularly in the E364Q mutant (Fig. 4C). Deletion of PsbV reduced fluorescence yield; this effect was enhanced by the Glu364 to Gln mutation in the E364Q:ΔPsbV double mutant. Measurements of low-temperature (77 K) fluorescence reflected similar differences between strains (Fig. S3), wherein fluorescence at pH 7.5 with 440 nm (targeting chlorophyll) and 580 nm (targeting phycobilisomes) excitation wavelengths reflected a reduction in assembled PS II and decreased accessory pigment coupling, respectively, in ΔPsbV and E364Q:ΔPsbV cells.

The net effect of PS II function in terms of electron transport to PS I can be inferred from analysis of P_{700} oxidation kinetics (Fig. 4D). Actinic illumination of dark-adapted cells results in a prompt change in absorbance in the near-infrared due to oxidation of P_{700}, which appears as a signal increase. Quenching of the signal then occurs due to a reduction in PS I by electron transport from PS II and/or cyclic electron transport *via* the cytochrome b_6f complex [39]. At pH 10.0, enhanced electron transport to PS I was observed in all strains relative to pH 7.5, with greater and generally more rapid quenching of P_{700}^+ after ~ 0.5 s. In E364Q cells, P_{700}^+ was apparently quenched more rapidly than in the wild-type, but deletion of PsbV both slowed and reduced the ability of electron transport to reduce P_{700}^+. This effect was greater in the E364Q:ΔPsbV double mutant, and it is noted that the limited variable chlorophyll fluorescence and P_{700}^+ quenching observed in these experiments both indicate functional electron transport in this mutant, but this is presumably insufficient to maintain pH 7.5 photoautotrophic growth.

Discussion

The Glu364 to Gln substitution affects PS II electron transfer processes, due to an effect on Y_D

Previous studies of loop E in CP47 identified amino acid residues that are now known to be located adjacent to Y_D [3,4,16] that were important for PS II assembly and function [19,45]. Among these a Glu364 to Gln substitution in CP47 appeared to produce only a minor phenotype, but the inability of an E364Q:ΔPsbV double mutant to grow photoautotrophically indicated the importance of this residue [20,21]. Although the Glu364 to Gln substitution did not substantially affect growth and oxygen evolution in the earlier studies, this study has unmasked potentially deleterious changes in PS II electron transfer processes in the E364Q strain, which we attribute to alterations in the H-bonding network around Y_D (Fig. 1). The striking increase in TL yield in the E364Q mutant (Fig. 2A,C; Table 2) suggests an increased probability that P_{680}* is repopulated during charge recombination in this strain with the likely consequence that the efficiency of nonradiative charge recombination would be reduced [34]. This might arise as a result of a destabilization of the interaction of D2 Arg294 with D2 His189 in the E364Q mutant modifying the formation of the neutral radical ($Y_D^{\cdot}$). Such a situation would reduce the

capacity of Y_D to reduce $P680^+$ and could increase C band emission, as well as B and Q band emissions, in the E364Q strain. Certainly, an increased overall TL emission from E364Q cells compared to wild-type points to modified redox potentials for specific S states or for the quinone electron acceptors resulting in altered stabilization of the $S_2Q_B^-$/$S_2Q_A^-$ states. However, a shift in TL peak temperatures in E364Q cells in both the presence and absence of DCMU points to a change on the donor side of PS II rather than an alteration in the vicinity of Q_A or Q_B [46].

A perturbed H-bonding network destabilizes Y_D and alters the dark equilibration of the S states

The increased amplitude of the C band indicates the enhanced formation of $Y_D^{(ox)}Q_A^-$ by the Glu364 to Gln substitution. In addition, in the oxygen yield measurements (Fig. 4A,B), an apparent shift toward the S_0 state following a brief (~ 5 min) dark adaption in the photoautotrophically grown E364Q cells and in the E364Q:ΔPsbV strain was evident, particularly in the double mutant, and this could also arise from altered conformation of the Y_D pocket by perturbation of the H-bond network that ordinarily links Glu364 to His_D (*via* D2 Arg294), affecting the proton transfer-coupled formation of $Y_D^{\cdot}$ [8–10,17]. This would lead to an increased fraction of centers in S_{OYD} after dark adaptation by reduction in the relative proportion of S_1Y_D in favor of $S_0Y_D^{(ox)}$. Or, formation of an unstable S_1Y_D would yield OEC centers that become S_2Y_D following a flash but that recombine to $S_1Y_D^{(ox)}$ rapidly, perhaps within the time scale of the Joliot electrode flash frequency [13]. The enhancement of TL emission arising from $Y_D^{(ox)}Q_A^-$ in the Glu364 to Gln mutants is consistent with this hypothesis; rapid decay of S_2 to S_1 following a flash would yield an increase in $Y_D^{(ox)}$ as the donor side recombination partner for acceptor side Q_A^-, which cannot recombine with S_1. Deletion of PsbV in *Thermosynechococcus elongatus* also resulted in an increase in the fraction of centers in the dark S_0 state in another study, prompting the suggestion that PsbV binding might also affect Y_D oxidation [47]; this would imply a twofold effect on Y_D in the E364Q:ΔPsbV mutant.

External pH affects electron transfer processes within PS II in intact cells

The external pH affected TL, variable chlorophyll fluorescence induction, and the chlorophyll fluorescence decay kinetics following a single actinic flash in all *Synechocystis* 6803 strains, including the wild-type. Likewise, the combined effect of linear and cyclic electron transfer on $P700^+$ rereduction was enhanced at pH 10.0 relative to pH 7.5 (Fig. 4D). This is in spite of the prevailing theory that the thylakoid lumen is approximately 2 pH units lower than the cytosolic pH [48,49], which is well buffered, varying between pH ~ 6.8–7.2 in *Synechocystis* 6803 at an external pH of 8.0–10.0, respectively [50]. In isolated thylakoids, TL analysis indicates that $Y_D^{(ox)}Q_A^-$ stability increases from pH ~ 7.5 to ~ 10.0 [51], and our results indicate $Y_D^{(ox)}Q_A^-$ stability was also potentially stabilized in wild-type, as judged by the increased amplitude for the C band in the presence of DCMU and an increase in T_{max} in the absence of DCMU (Table 2). The impact of pH on $Y_D^{(ox)}Q_A^-$ stability was most evident in E364Q cells whereupon increasing the pH from 7.5 to 10.0 increased both the T_{max} and amplitude of the C band both in the presence and absence of DCMU (Table 2). Additionally, an increase in both the B and Q band T_{max} values for E364Q and E364Q:ΔPsbV cells at pH 10.0 also indicates that the external pH can influenced the stability of both $S_2Q_A^-$ and $S_2Q_B^-$. It is possible that despite the buffering capacity of the cytosol the thylakoid lumen does become more alkaline when cells are in pH 10.0 media. This could help maintain the S_1/S_0 ratio in the dark to favor a more stable OEC [10,14]. This might counteract the effects of the Glu364 to Gln mutation and/or the loss of PsbV leading to the enhanced rates of electron transport observed in Fig. 4D and the reactivation of photoautotrophic growth in E364Q:ΔPsbV cells at pH 10.0 [23].

Acknowledgements

We thank Dr Simon A. Jackson for assistance with use of the Joliot electrode, and László Sass for assistance with the operation of TL-measuring equipment and the analysis of the O_2 flash patterns. JNM was supported by the Senior Smeaton Prize in Experimental Science at the University of Otago. The laboratory of IV is supported by grant number NKFI-H (NN-110960) and GINOP-2.3.2-15-2016-00001.

Author contributions

JNM, IV, TCS, and JER designed the experiments, and JNM and SK conducted the experimental work. JNM analyzed the data and wrote the manuscript; all authors contributed to discussions about data interpretation, and had direct input on manuscript content and editing, before submission.

References

1 Shen J-R (2015) The structure of Photosystem II and the mechanism of water oxidation in photosynthesis. *Annu Rev Plant Biol* **66**, 23–48.

2 Bricker TM, Roose JL, Fagerlund RD, Frankel LK and Eaton-Rye JJ (2012) The extrinsic proteins of Photosystem II. *Biochim Biophys Acta* **1817**, 121–142.

3 Ferreira KN, Iverson TM, Maghlaoui K, Barber J and Iwata S (2004) Architecture of the photosynthetic oxygen-evolving complex. *Science* **303**, 1831–1838.

4 Umena Y, Kawakami K, Shen J-R and Kamiya N (2011) Crystal structure of oxygen-evolving Photosystem II at a resolution of 1.9 Å. *Nature* **473**, 55–60.

5 Ago H, Adachi H, Umena Y, Tashiro T, Kawakami K, Kamiya N, Tian L, Han G, Kuang T, Liu Z *et al.* (2016) Novel features of eukaryotic Photosystem II revealed by its crystal structure analysis from a red alga. *J Biol Chem* **291**, 5676–5687.

6 Wei X, Su X, Cao P, Liu X, Chang W, Li M, Zhang X and Liu Z (2016) Structure of spinach Photosystem II LHCII supercomplex at 3.2 Å resolution. *Nature* **536**, 69–74.

7 Vinyard DJ, Ananyev GM, Dismukes CG and Charles Dismukes G (2013) Photosystem II: the reaction center of oxygenic photosynthesis. *Annu Rev Biochem* **82**, 577–606.

8 Nakamura S and Noguchi T (2015) Infrared detection of a proton released from tyrosine Y_D to the bulk upon its photo-oxidation in Photosystem II. *Biochemistry* **54**, 5045–5053.

9 Saito K, Rutherford AW and Ishikita H (2013) Mechanism of tyrosine D oxidation in Photosystem II. *Proc Natl Acad Sci U S A* **110**, 7690–7695.

10 Styring S, Sjöholm J and Mamedov F (2012) Two tyrosines that changed the world: Interfacing the oxidizing power of photochemistry to water splitting in Photosystem II. *Biochim Biophys Acta* **1817**, 76–87.

11 Kok B, Forbush B and McGloin M (1970) Cooperation of charges in photosynthetic O_2 evolution - I. A linear four step mechanism. *Photochem Photobiol* **11**, 457–475.

12 Rutherford AW, Boussac A and Faller P (2004) The stable tyrosyl radical in Photosystem II: Why D? *Biochim Biophys Acta* **1655**, 222–230.

13 Vass I, Deák Z and Hideg É (1990) Charge equilibrium between the water-oxidizing complex and the electron donor tyrosine-D in Photosystem II. *Biochim Biophys Acta* **1017**, 63–69.

14 Vass I and Styring S (1991) pH-Dependent charge equilibria between tyrosine-$_D$ and the S states in photosystem II. Estimation of relative midpoint redox potentials. *Biochemistry* **30**, 830–839.

15 Eaton-Rye JJ and Putnam-Evans C (2005) The CP47 and CP43 core antenna components. In Photosystem II: The Light-Driven Water:Plastoquinone Oxidoreductase (Wydrzynski TJ and Satoh K eds), Advances in Photosynthesis and Respiration, Vol. **22**, pp. 45–70. Springer, Dordrecht, The Netherlands.

16 Suga M, Akita F, Hirata K, Ueno G, Murakami H, Nakajima Y, Shimizu T, Yamashita K, Yamamoto M, Ago H *et al.* (2015) Native structure of Photosystem II at 1.95 Å resolution viewed by femtosecond X-ray pulses. *Nature* **517**, 99–103.

17 Sjöholm J, Ho F, Ahmadova N, Brinkert K, Hammarström L, Mamedov F and Styring S (2017) The protonation state around $Tyr_D/Tyr_D^{\cdot}$ in Photosystem II is reflected in its biphasic oxidation kinetics. *Biochim Biophys Acta* **1858**, 147–155.

18 Clarke SM and Eaton-Rye JJ (1998). Characterization of the double mutant FF362,363RR in loop E of the Photosystem II chlorophyll-binding protein CP47. In Photosynthesis: Mechanisms and Effects (Garab G, ed.), Vol. **II**, pp. 1459–1462. Kluwer Academic Publishers, Dordrecht, the Netherlands.

19 Clarke SM and Eaton-Rye JJ (1999) Mutation of Phe-363 in the Photosystem II protein CP47 impairs photoautotrophic growth, alters the chloride requirement, and prevents photosynthesis in the absence of either PSII-O or PSII-V in *Synechocystis* sp. PCC 6803. *Biochemistry* **38**, 2707–2715.

20 Morgan TR, Shand JA, Clarke SM and Eaton-Rye JJ (1998) Specific requirements for cytochrome c_{550} and the manganese-stabilizing protein in photoautotrophic strains of *Synechocystis* sp. PCC 6803 with mutations in the domain Gly-351 to Thr-436 of the chlorophyll-binding protein CP47. *Biochemistry* **37**, 14437–14449.

21 Putnam-Evans C, Wu J and Bricker TM (1996) Site-directed mutagenesis of the CP47 protein of Photosystem II: alteration of conserved charged residues which lie within lethal deletions of the large extrinsic loop E. *Plant Mol Biol* **32**, 1191–1195.

22 Roose JL, Frankel LK, Mummadisetti MP and Bricker TM (2016) The extrinsic proteins of Photosystem II: update. *Planta* **243**, 889–908.

23 Eaton-Rye JJ, Shand JA and Nicoll WS (2003) pH-dependent photoautotrophic growth of specific Photosystem II mutants lacking lumenal extrinsic polypeptides in *Synechocystis* PCC 6803. *FEBS Lett* **543**, 148–153.

24 Summerfield TC, Shand JA, Bentley FK and Eaton-Rye JJ (2005) PsbQ (Sll1638) in *Synechocystis* sp. PCC 6803 is required for Photosystem II activity in specific mutants and in nutrient-limiting conditions. *Biochemistry* **44**, 805–815.

25 Summerfield TC, Crawford TS, Young RD, Chua JP, Macdonald RL, Sherman LA and Eaton-Rye JJ (2013) Environmental pH affects photoautotrophic growth of *Synechocystis* sp. PCC 6803 strains carrying mutations

in the lumenal proteins of PS II. *Plant Cell Physiol* **54**, 859–874.
26 Summerfield TC, Eaton-Rye JJ and Sherman LA (2007) Global gene expression of a ΔPsbOΔPsbU mutant and a spontaneous revertant in the cyanobacterium *Synechocystis* sp. strain PCC 6803. *Photosynth Res* **94**, 265–274.
27 Summerfield TC, Winter RT and Eaton-Rye JJ (2005) Investigation of a requirement for the PsbP-like protein in *Synechocystis* sp. PCC 6803. *Photosynth Res* **84**, 263–268.
28 Morris JN, Eaton-Rye JJ and Summerfield TC (2016) Environmental pH and the requirement for the extrinsic proteins of Photosystem II in the function of cyanobacterial photosynthesis. *Front Plant Sci* **7**, 1135. https://doi.org/10.3389/fpls.2016.01135
29 Bricker TM, Mummadisetti MP and Frankel LK (2015) Recent advances in the use of mass spectrometry to examine structure/function relationships in Photosystem II. *J Photochem Photobiol, B* **152**, 227–246.
30 Rippka R, Deruelles J, Waterbury JB, Herdman M and Stanier RY (1979) Generic assignments, strain histories and properties of pure cultures of cyanobacteria. *J Gen Microbiol* **111**, 1–61.
31 Eaton-Rye JJ (2011). Construction of gene interruptions and gene deletions in the cyanobacterium *Synechocystis* sp. strain PCC 6803. *Methods Mol Biol* **684**, 295–312.
32 Ducruet JM and Vass I (2009) Thermoluminescence: experimental. *Photosynth Res* **101**, 195–204.
33 Vass I, Horvath G, Herczeg T and Demeter S (1981) Photosynthetic energy conservation investigated by thermoluminescence. *Biochim Biophys Acta* **634**, 140–152.
34 Cser K and Vass I (2007) Radiative and non-radiative charge recombination pathways in Photosystem II studied by thermoluminescence and chlorophyll fluorescence in the cyanobacterium *Synechocystis* 6803. *Biochim Biophys Acta* **1767**, 233–243.
35 Joliot P and Joliot A (1968) A polarographic method for detection of oxygen production and reduction of Hill reagent by isolated chloroplasts. *Biochim Biophys Acta* **153**, 625–634.
36 Jackson SA and Eaton-Rye JJ (2015) Characterization of a *Synechocystis* sp. PCC 6803 double mutant lacking the CyanoP and Ycf48 proteins of Photosystem II. *Photosynth Res* **124**, 217–229.
37 Deák Z, Sass L, Kiss É and Vass I (2014) Characterization of wave phenomena in the relaxation of flash-induced chlorophyll fluorescence yield in cyanobacteria. *Biochim Biophys Acta* **1837**, 1522–1532.
38 Vass I, Kirilovsky D and Etienne AL (1999) UV-B radiation-induced donor- and acceptor-side modifications of Photosystem II in the cyanobacterium *Synechocystis* sp. PCC 6803. *Biochemistry* **38**, 12786–12794.
39 Klughammer C and Schreiber U (1994) An improved method, using saturating light-pulses, for the determination of Photosystem-I quantum yield via P_{700}^{+}-absorbancy changes at 830 nm. *Planta* **192**, 261–268.
40 Arnold W and Sherwood HK (1957) Are chloroplasts semiconductors? *Proc Natl Acad Sci U S A* **43**, 105–114.
41 Sane PV (2004). Thermoluminescence: a technique for probing Photosystem II. *Methods Mol Biol* **274**, 229–248.
42 Robinson HH and Crofts AR (1983) Kinetics of the oxidation–reduction reactions of the Photosystem II quinone acceptor complex, and the pathway for deactivation. *FEBS Lett* **153**, 221–226.
43 Kaňa R, Kotabová E, Komárek O, Šedivá B, Papageorgiou GC, Govindjee and Prášil O (2012) The slow S to M fluorescence rise in cyanobacteria is due to a state 2 to state 1 transition. *Biochim Biophys Acta* **1817**, 1237–1247.
44 Papageorgiou GC and Govindjee (2011) Photosystem II fluorescence: slow changes - scaling from the past. *J Photochem Photobiol, B* **104**, 258–270.
45 Eaton-Rye JJ and Vermaas WFJ (1991) Oligonucleotide-directed mutagenesis of *psbB*, the gene encoding CP47, employing a deletion mutant strain of the cyanobacterium *Synechocystis* sp. PCC 6803. *Plant Mol Biol* **17**, 1165–1177.
46 Vass I and Govindjee (1996) Thermoluminescence from the photosynthetic apparatus. *Photosynth Res* **48**, 117–126.
47 Kirilovsky D, Roncel M, Boussac A, Wilson A, Zurita JL, Ducruet J-M, Bottin H, Sugiura M, Ortega JM and Rutherford AW (2004) Cytochrome c_{550} in the cyanobacterium *Thermosynechococcus elongatus*: study of redox mutants. *J Biol Chem* **279**, 52869–52880.
48 Belkin S, Mehlhorn RJ and Packer L (1987) Proton gradients in intact cyanobacteria. *Plant Physiol* **84**, 25–30.
49 Belkin S and Packer L (1988) Determination of pH gradients in intact cyanobacteria by electron spin resonance spectroscopy. *Methods Enzymol* **167**, 677–685.
50 Jiang HB, Cheng HM, Gao KS and Qiu BS (2013) Inactivation of Ca^{2+}/H^{+} exchanger in *Synechocystis* sp. strain PCC 6803 promotes cyanobacterial calcification by upregulating CO_2-concentrating mechanisms. *Appl Environ Microbiol* **79**, 4048–4055.
51 Vass I and Inoue Y (1986) pH dependent stabilization of $S_2Q_A^-$ and $S_2Q_B^-$ charge pairs studied by thermoluminescence. *Photosynth Res* **10**, 431–436.

52 DeLano WL (2001) The PyMOL Molecular Graphics System. DeLano Scientific, Palo Alto, CA.
53 Morris JN, Crawford TS, Jeffs A, Stockwell PA, Eaton-Rye JJ and Summerfield TC (2014) Whole genome re-sequencing of two "wild-type" strains of the model cyanobacterium *Synechocystis* sp. PCC 6803. *NZ J Bot* **52**, 36–47.
54 Morris JN, Eaton-Rye JJ and Summerfield TC (2017) Phenotypic variation in wild-type substrains of the model cyanobacterium *Synechocystis* sp. PCC 6803. *NZ J Bot* **55**, 25–35.
55 Delrieu M-J (1974) Simple explanation of the misses in the cooperation of charges in photosynthetic O_2 evolution. *Photochem Photobiol* **20**, 441–454.

Supporting information

Additional supporting information may be found online in the Supporting Information section at the end of the article.

Fig. S1. Comparison of average experimental and average fitted flash-induced oxygen evolution data for mixotrophically grown cells.
Fig. S2. Comparison of average experimental and average fitted flash-induced oxygen evolution data for autotrophically grown cells.
Fig. S3. Low-temperature fluorescence emission.